Transactions, SMiRT-23
Manchester, United Kingdom - August 10-14, 2015
Division VI
Paper ID: 708

SHEAR STRENGTH AND BEHAVIOR OF RC STRUCTURES WITH T-HEADED BARS FOR SHEAR REINFORCEMENT

Yuxing Yang[1], Amit Varma[2], Michael Kreger[3], and Thomas Bradt[4]

[1] PhD candidate, Purdue University, USA
[2] Professor, Purdue University, USA
[3] Professor, Chair in Civil Engineering, The University of Alabama, USA
[4] Research Engineer, Bowen Laboratory, Purdue University, USA

ABSTRACT

The design of concrete structures for safety-related nuclear facilities is governed by demands calculated for load combinations involving safe shutdown earthquake (SSE). Excessive amounts of longitudinal and transverse reinforcement (in excess of 2% reinforcement ratio) are required to provide essentially elastic behavior for SSE and resist the design demands. Additionally, conventional shear reinforcement (single-leg ties) with 90° and 135° hooks at alternate ends are required for seismic detailing. All these requirements lead to rebar congestion, and make conventional single-leg ties difficult to install in reinforced concrete (RC) structures. T-headed shear bars are being considered to resolve this issue. These consist of deformed rebars with T- heads in the form or welded or threaded rebar terminators with bearing area greater than or equal to four times the rebar area. However, experimental data regarding the shear strength of RC structures with T-headed shear bars is lacking.

This paper presents the results of experimental investigations conducted to evaluate the shear behavior and strength of RC beams using T-headed shear bars. The behavior of specimens with three different depths of 18 in., 24 in., and 36 in. and three different T-headed bar sizes (#5, #7, and #9) are investigated and compared with the behavior of companion specimens with conventional stirrups. Experimental results include the shear force-displacement behavior of the beam, shear force-strain responses of the longitudinal and shear reinforcement, and observations of concrete cracking and shear failure. Experimental results and observations indicate that specimens using T-headed bars had slightly better behavior and shear strength than the companion specimens using conventional stirrups, which opened up close to failure for some tests. The out-of-plane shear strength of specimens with T-heads can be predicted conservatively using the current ACI 349-01 code equations.

INTRODUCTION

Sponsored by Westinghouse Electric Company (WEC), the shear strength of RC structures with T-headed bars as shear reinforcement is investigated in this study. Previous researches from Kim et, al (2004) and Yang et, al (2010) on T-headed bars paid limited attention to the effect of dimension change, extremely high reinforcing ratio, and whether designers could use code equations to conservatively predict the shear strength of flexural elements incorporating T-headed bars. This paper presents the investigation of shear strength and behavior of RC beams with T-headed bars as shear reinforcement. Twelve specimens were tested to investigate whether ACI 349 code provisions can conservatively predict the shear strength. Parameters such as dimension change and high reinforcing ratio are considered. Companion specimens with conventional stirrups with 90° and 135° hooks were also tested to compare with the results.

T-headed bars used in this study, as shown in Figure 1 (radii of circles is 1 in. and 2 in., respectively), consist of a pre-threaded straight bar and two mechanical anchors manufactured by Erico (2009). The head area of the anchors meets five times the bar area. Safety-related nuclear construction

requires heavily reinforced members to provide elastic behaviour, therefore, the placement of conventional single-leg ties can be difficult due to fabrication tolerances and interruptions of longitudinal reinforcement. Placement of single-leg ties can be simplified using T-headed bars due to its shape and dimension that is free of hooks and bends.

To investigate the effectiveness of T-headed bars for use as ties in RC structures for safety-related nuclear facilities, T-headed bars are used as shear reinforcement in beam specimens to investigate the ability of T-heads to sufficiently anchor the bars to permit development of their yield strength. This project will experimentally evaluate and compare the shear behavior and strength of RC beams with T-headed bars with beams with conventional stirrups. The parameters included in the experimental investigation are: (i) the section depth, (ii) the diameter of the T-headed shear bars, and (iii) the shear span-to-depth ratio. All the specimens utilize #11 longitudinal reinforcement with adequate development length, and the maximum spacing of shear reinforcement permitted by ACI 349 Code provisions.

TEST PROGRAM

Specimen

Test specimens are doubly-reinforced full-scale beams of three different thicknesses. The number and distribution of flexural and shear reinforcement in the specimens were designed so that shear failure would occur before flexural capacity is reached. A total of twelve specimens were tested in four groups of three specimens each. The test matrix is summarized in Table 1. The specimens in Groups 1, 2, 3, and 4 have section depths (h) of 18 in., 24 in., and 36 in., respectively, and utilize #5, #7, #9, and #5 shear reinforcement, respectively. Groups 1-3 include replicate specimens (noted with letter "R") with T-headed bars as shear reinforcement (noted with letter "T"), and an equivalent (third) specimen with stirrups (noted with letter "S") to compare directly with the two specimens with T-headed bars. T-headed bars are anchored in the specimens using D6 LENTON® terminators.

The specimens within each of the Groups 1-3 have the same: (i) number and distribution of longitudinal reinforcement in the specimen cross-section, (ii) shear span-to-depth (a/h) ratio of 2.5, (iii) shear reinforcement area and spacing, and (iv) cross-section depth. The lengths of the specimens have been designed to fully develop the longitudinal reinforcement in the end regions of each beam. Group 4 includes three 24-in. deep specimens with T-headed bars as shear reinforcement. The pair of replicate specimens in Group 4 have a shear span-to-depth ratio of 3.5, and one specimen has a shear span-to-depth ratio of 2.5 to compare directly with the other two specimens and evaluate the effects of shear span-to-depth ratio on shear strength.

Material

The material properties were determined by conducting tests in accordance with corresponding ASTM standards. Concrete cylinder compression tests were conducted on the 3rd, 7th, and 28th days after casting and on the day of testing. Three cylinders were tested for each test. All cylinders tested were 4 in. in diameter and 8 in. in height. Specimen testing was performed when the concrete strength reached approximately 4000 psi. A summary of the material properties for steel reinforcement and concrete is presented in Table 2.

Test Setup and Loading Protocol

The beam specimens were tested using a four-point bending test setup so that applied loads resulted in uniform shear over the shear span (between loading point and support), and uniform moment between the loading points, as shown in Figure 2. The distance between two concrete blocks (supports) changes as required based on different shear span lengths of each specimen. As shown, the test setup consists of two loading frames. For each loading frame, two W-shape columns connected with a loading

beam. A 500 kip capacity hydraulic ram is attached to each loading beam. The ram applies force to a load spreader beam, which distributes the load to the top face of the specimen.

The testing procedure used in this study is based on the cyclic testing procedure aimed at evaluating the seismic performance of structural components (Krawinkler, 2009). However, reversed cyclic loading could not be performed due to the limitations of the test setup and hydraulic equipment. Loading-unloading cycles were conducted at 25%, 50%, and 75% of V_n^{exp} to facilitate concrete cracking and obtain stiffness response of the cracked specimens without the influence of permanent displacements due to cracking. The expected shear strength (V_n^{exp}) is calculated using the ACI 349 code recommendation, while using measured steel and concrete material strengths as available and assuming ϕ = 1.0.

The reinforcement layout of specimens in each group is shown in Figure 3. For companion specimens with conventional stirrups, T-headed bars were replaced by stirrups, and the corresponding cross-section layout remained unchanged. The total length of specimens in Group 1, 2, and 4 is 24 ft., and the total length of specimens in Group 3 is 27 ft. The loading points are 4 ft. apart for specimens in Group 1, 2, and 4. The loading points are 6 ft. apart for specimens in Group 3. For specimens with T-headed bars, stirrups were replaced by T-headed bars in the shear reinforcement layout, and the corresponding spacing remained unchanged.

TEST RESULTS

Similar experimental behavior was observed in all twelve specimens. In this section, representative behavior is presented and compared between Specimen 36-9T, which uses T-headed bars as shear reinforcement, and its companion specimen 36-9S, which uses conventional stirrups. The experimental behavior includes shear force-deflection responses, strain distribution in shear reinforcement, moment-curvature response, flexural strain profile, and crack pattern at failure.

Shear Force-Deflection Response

The shear force-deflection (V - Δ) response for 36-9T and 36-9S is shown in Figure 4 (a) and Figure 4 (b), respectively. The figures include the measured V - Δ responses for all four cycles of loading, up to 25%, 50%, and 75% of V_n^{exp}, and the final loading cycle up to failure. The secant stiffness of each specimen (K_{sec}^{test}) was calculated based on ⅔V_{test} and the corresponding deflection (Δ_1). After the peak load, the specimen demonstrated reduced capacity and experienced a shear-compression failure. The specimen was unloaded before catastrophic failure that could have damaged instrumentation located beneath the specimen. Figure 4 shows that the experimental shear capacities (V_{test}) of 36-9T and 36-9S were 498 kips and 439 kips, respectively. The midspan deflections at failure (Δ_{test}) were 1.09 in. and 0.95 in., respectively. It was observed that 36-9T had 59 kips more shear capacity and 0.14 in. more deflection capacity than 36-9S. Figure 4 also shows that 36-9T and 36-9S had similar stiffness response. The test K_{sec}^{test} of 36-9T and 36-9S was 511 kips/in and 514 kips/in, respectively. The value of V_{test}, Δ_{test}, and K_{sec}^{test} of all specimens in the test matrix are summarized in Table 3.

Strain Distribution in Shear Reinforcement

The strain distribution in shear reinforcement in the failure shear span of the first two loading cycles and full history for 36-9T and 36-9S is shown in Figure 5. Both flexural and shear crack openings (diagonal cracking across the shear span) in specimen shear spans were observed. Cracking was reflected in the measured strain responses by a large horizontal strain increment at a certain load stage. For 36-9T, Figure 5 (b) indicates crack opening by S13 and S14, and S15 and S16 at loads of approximately 160 kips, 170 kips (first shear crack opening), and 200 kips in the South shear span. For 36-9S, Figure 5 (c) shows that crack opening was indicated by S9 and S10 measured strains at loads of 125 kips, 150 kips,

170 kips (first shear crack opening), and 180 kips in the North shear span. Upon specimen failure, strain values consistently greater than 0.01 were measured by strain gages S13 to S16, as shown in Figure 5 (d), and S9, as shown in Figure 5 (e), indicating opening of major diagonal cracks. The high strain values in the figures indicate that a substantial portion of the shear force was transferred from concrete to the steel reinforcement at the location of these strain gages by the time specimen failure occurred.

Moment-Curvature Response

The predicted M-ϕ relationships are compared with M-ϕ responses inferred from measured rotation data, and the results are shown in Figure 6. The moment from test was calculated simply as shear force (V) times shear span (a), and the curvature was calculated using rotation data measured from two loading points (CM3 and CM12). Prediction of the moment-curvature relationship was based on assumptions of strain compatibility between the steel and concrete, an elastic-plastic stress-strain relationship for reinforcement, Popovics' (1973) stress-strain relationship for concrete in compression, and zero tensile stress capacity for concrete in tension. The cross-section was discretized into a grid of steel and concrete fibers with associated areas and distances from the centroidal axis. The extreme fiber compressive strain (ϵ_c) was increased gradually, and section force equilibrium was established to locate the neutral axis. The moment (M) and curvature (ϕ) for the cross-section were then obtained from integration.

Figure 6 (a) and Figure 6 (b) show that the predicted M-ϕ relationships were in reasonable agreement with the inferred responses. The maximum difference in curvature between predicted and that inferred from test data is within 1.0×10^{-4} 1/ft. There are no test data shown in the inelastic region of the M-ϕ predicted response because specimens failed in shear before significant inelastic response occurred.

Midspan Flexural Strain Profile

The predicted midspan cross-section flexural strain profiles are compared with measured strains, and the results are shown in Figure 7. The calculated strain profiles and measured strains at 25% of V_n^{exp}, 50% of V_n^{exp}, 75% of V_n^{exp}, and at failure are compared. The measured strains were obtained from concrete strain gages CS1 and CS2 and steel strain gages S1 through S8, as shown in Figure 5 (a). The calculated strain profiles are obtained from M-ϕ analysis. In the figures, the calculated strain distributions for 25% of V_n^{exp}, 50% of V_n^{exp}, 75% of V_n^{exp}, and at failure are straight lines because the assumption of plane sections remaining plane was invoked during the M-ϕ analysis. Figure 7 (a) and Figure 7 (b) shows that the assumption of plane sections remaining plane was incorrect yet predicted strain profiles agreed reasonably well with measured strains. Figure 7 (a) and Figure 7 (b) shows that the maximum difference between predicted and measured strains in layers of steel reinforcement is 2.7×10^{-4}, and the maximum difference between predicted and measured concrete strains at the extreme concrete compression fiber is 2.2×10^{-4}.

Crack Pattern

Photographs of cracks on specimen shear spans at V_{test} are shown in Figure 8 for 36-9T and 36-9S. For 36-9T, Figure 8 (a) shows that failure occurred in the South shear span. Critical shear cracks propagated from the loading point to the support. The first shear crack was observed at a load of about 170 kips. For 36-9S, Figure 8 (b) shows that failure occurred in the North shear span. The critical shear crack propagated from the loading point to the support with a much wider crack width than that observed for 36-9T and 36-9TR. Concrete cover was crushed near the North loading point. Horizontal cracks propagated at the bottom of the specimen where tension layers of longitudinal reinforcement were located, indicating concrete splitting in the plane of steel reinforcement. The first shear crack was

observed at a load of about 170 kips. Figure 8 (c) and Figure 8 (d) shows that concrete cover on the specimen top and bottom faces was pushed off by the 90° bend in stirrups trying to straighten.

SHEAR STRENGTH COMPARISON

The ACI 349 requirements were used to predict the shear strength of specimens in the test matrix. The ACI 349 Code provisions are a combination of an empirical formula and an equilibrium model based on an analogy. The nominal shear strength of non-prestressed concrete beams with shear reinforcement is taken as $V_n = V_c + V_s$, where V_c represents a concrete contribution as a function of concrete uniaxial compressive strength, and V_s represents strength provided by shear reinforcement. For concrete contribution, V_c is an empirical formula based on a reasonable lower bound of test results of hundreds of concrete beams without shear reinforcement, and is suggested as Equation (1). The strength provided by shear reinforcement V_s with vertical bars represents the truss capacity in shear derived from the equilibrium condition by summing the vertical forces on an inclined crack free-body diagram with an assumed fixed inclination angle of 45°. The expression is shown as Equation (2).

$$V_c = 2\sqrt{f_c'}\, b_w d \tag{1}$$

$$V_s = \frac{A_v f_y d}{s} \tag{2}$$

In Equation (1) and Equation (2), f_c' is the concrete compressive strength, b_w is the width of the member, d is the distance from extreme compression fiber to the centroid of tension reinforcement, A_v is the area of shear reinforcement, f_y is the yield strength of shear reinforcement, and s is the maximum spacing of shear reinforcement.

The test shear strength (V_{test}) of specimens in the test matrix is summarized in Figure 9 (a). The predicted shear strength (V_n^{exp}) of specimens was calculated using measured material properties shown in Table 2, and was compared with V_{test}. The results are summarized in Figure 9 (b) as the ratio of V_{test} to V_n^{exp}. Figure 9 (a) shows that specimens with T-headed bars have marginally higher shear strength than specimens with conventional stirrups. Specimens in Group 4 show that different shear span-to-depth ratio of 2.5 or 3.5 has little influence on the shear strength of specimens with T-headed bars. In Figure 9 (b), V_{test}/V_n^{exp} values for the specimens with T-headed bars show conservative predictions with an average of 1.19 and a standard deviation of 0.08. For companion specimens with conventional stirrups, ACI 349 provided reasonable strength prediction with a maximum error of 10%. It can be seen that for heavily RC members with T-headed bars, ACI 349 requirements can be used to predict the shear strength with reasonable conservatism.

CONCLUSION

This study presents the test program investigating the shear strength and behavior of RC structures using T-headed bars as shear reinforcement in safety-related nuclear facilities. Twelve full-scale specimens were fabricated and tested to experimentally investigate the shear strength and behavior of heavily RC beams with T-headed bars as shear reinforcement. Companion specimens with conventional stirrups were also tested and compared. From the test results of twelve specimens in this experimental investigation, specimens with T-headed bars have at least 7% higher shear capacity than specimens with conventional stirrups. There is no significant difference in behavior between specimens with T-headed bars and specimens with conventional stirrups, and between specimens with 2.5 *a/d* ratio and 3.5 *a/d* ratio. The conclusions are:

1. Specimens with T-headed bars as shear reinforcement had marginally better behavior and shear strength than the companion specimens with conventional stirrups.
2. Replacing conventional stirrups with T-headed bars as shear reinforcement doesn't have a detrimental influence on the behavior of the structure.
3. The shear strength of doubly reinforced (>2% tension and compression reinforcement ratio) concrete structures with T-headed bars as shear reinforcement can be predicted conservatively using ACI 349 code recommendation.

REFERENCES

ACI Committee 349 (2001), "Code Requirements for Nuclear Safety Related Concrete Structures (ACI 349-01)", American Concrete Institute, Farmington Hills, Mich., pp. 37

Erico International Cooperation (2009). "LENTON® TERMINATOR "D6" Embedment Anchor," Solon, Ohio, USA

Kim, Y. H., Yoon, Y. S., Cook, W. D., and Mitchell, D. (2004). "Repeated Loading Tests of Concrete Walls Containing Headed Shear Reinforcement" Journal of Structural Engineering (ASCE), 130, pp. 1233-1241

Krawinkler, H. (2009). "Loading Histories for Cyclic Tests in Support of Performance Assessment of Structural Components", Department of Civil and Environmental Engineering, Stanford University, Stanford, CA

Popovics, S. (1973). "A Numerical Approach to the Complete Stress-Strain Curve of Concrete." Cement and Concrete Research, Vol. 3, 583–599.

Yang, J.M., Min, K.H., Shin, H.O., and Yoon, Y.S. (2010). "The Use of T-headed Bars in High-Strength Concrete Members" Korea Concrete Institute, Proceedings of FraMCoS-7, May 23-28

Table 1: Test Matrix

Group	Specimen	Width, in	Depth, in	Shear Reinforcement	a/d Ratio
1	18-5T	36	18	#5 T-Head	2.5
	18-5TR				
	18-5S			#5 Stirrup	
2	24-7T		24	#7 T-Head	
	24-7TR				
	24-7S			#7 Stirrup	
3	36-9T		36	#9 T-Head	
	36-9TR				
	36-9S			#9 Stirrup	
4	24-5T-2.5		24	#5 T-Head	
	24-5T-3.5				3.5
	24-5TR-3.5				

Table 2: Material Properties

Group	Specimen	Average Concrete Strength, psi	Steel Reinforcement Strength, ksi		
		Test day	Flexure F_y (F_u)	T-headed bar F_y (F_u)	Stirrup F_y (F_u)
1	18-5T	5123	69.8 (97.5)	66.5 (92.2)	66.8 (104.9)
	18-5TR	4927			
	18-5S	4530			

Table 2: continued

Group	Specimen	Average Concrete Strength, psi	Steel Reinforcement Strength, ksi		
		Test day	Flexure F_y (F_u)	T-headed bar F_y (F_u)	Stirrup F_y (F_u)
2	24-7T	5417	70.1 (96.7)	67.9 (95.4)	67.9 (95.4)
	24-7TR	5380			
	24-7S	5555			
3	36-9T	5068	70.6 (96.0)	70.5 (102.7)	69.2 (100.5)
	36-9TR	4200			
	36-9S	4680			
4	24-5T-2.5	5293	69.7 (96.8)	69.1 (92.6)	N/A
	24-5T-3.5	4768			
	24-5TR-3.5	5450			

Table 3: Summary of V-Δ Response for Specimens in the Test Matrix

Specimen	V_{test}, kips	Δ_{test}, in	K_{sec}^{test}, kips/in	Specimen	V_{test}, kips	Δ_{test}, in	K_{sec}^{test}, kips/in
18-5T	276	0.58	526	36-9T	498	1.09	511
18-5TR	320	0.83	507	36-9TR	531	1.24	492
18-5S	257	0.58	653	36-9S	439	0.95	514
24-7T	419	0.78	775	24-5T-2.5	281	0.69	492
24-7TR	398	0.83	602	24-5T-3.5	254	0.91	331
24-7S	342	0.58	670	24-5TR-3.5	281	1.06	302

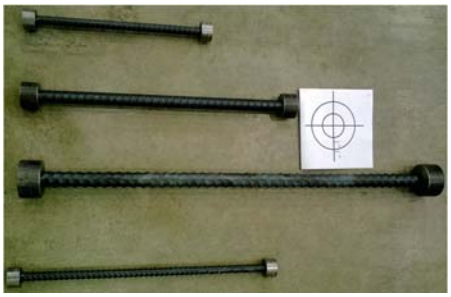

Figure 1. T-headed bars

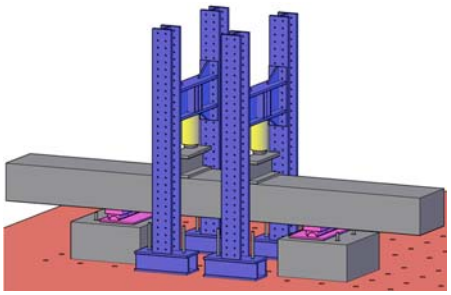

Figure 2. Test Setup

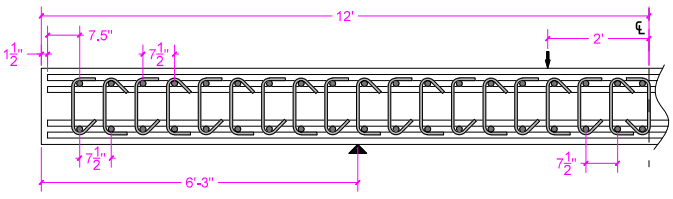

(a) Group 1

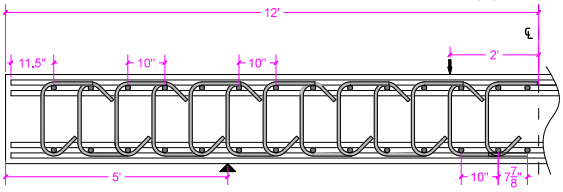

(b) Group 2

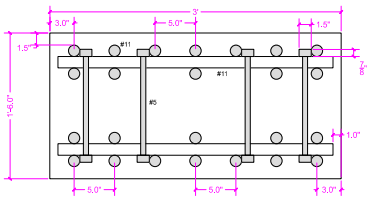

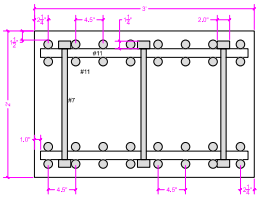

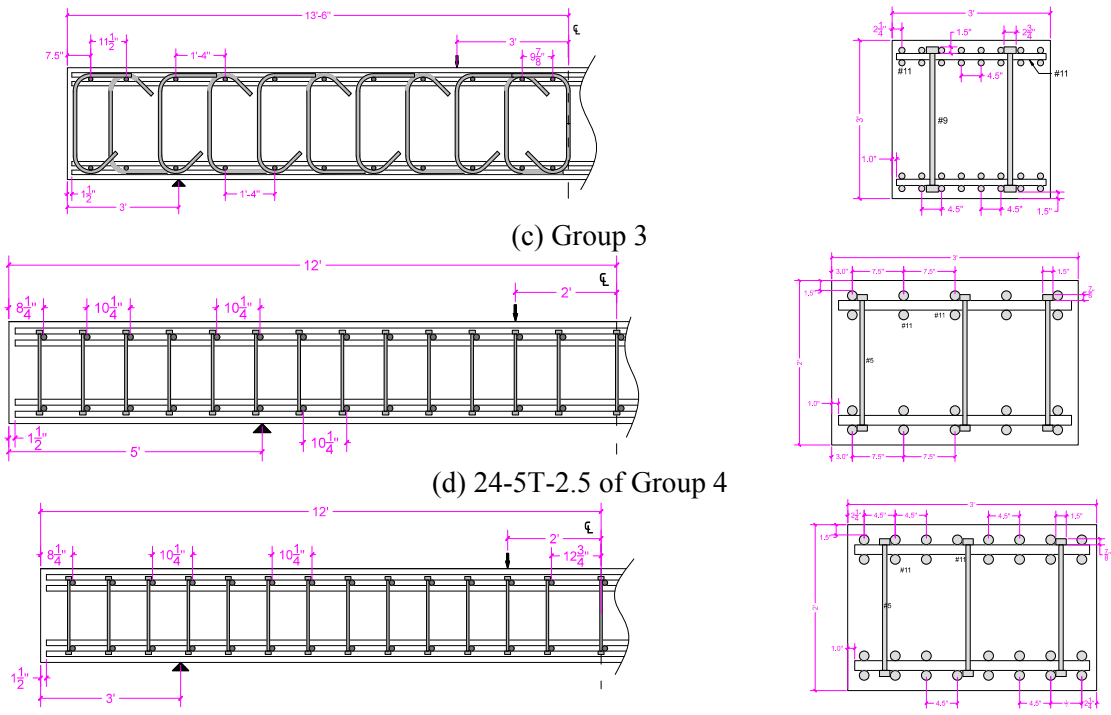

(c) Group 3

(d) 24-5T-2.5 of Group 4

(e) 24-5T-3.5 of Group 4

Figure 3. Specimen Reinforcement Layout

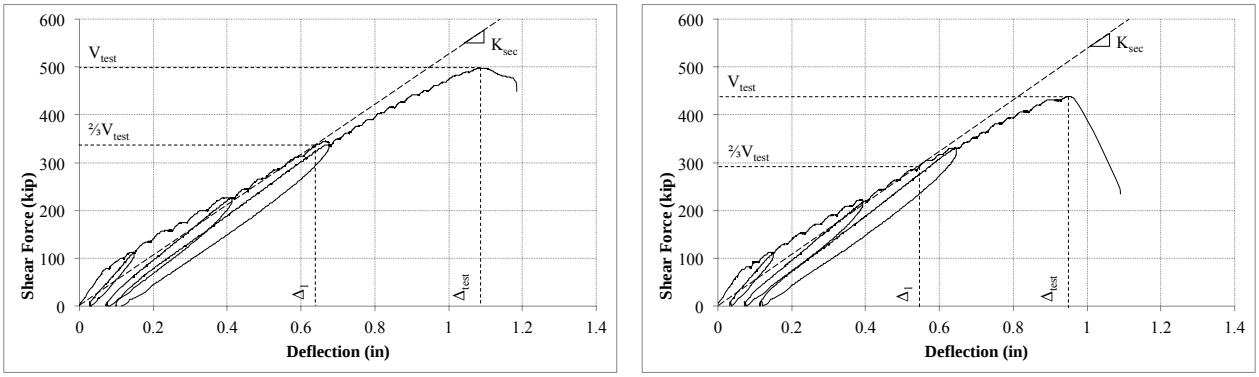

(a) 36-9T

(b) 36-9S

Figure 4. Shear Force-Deflection Response

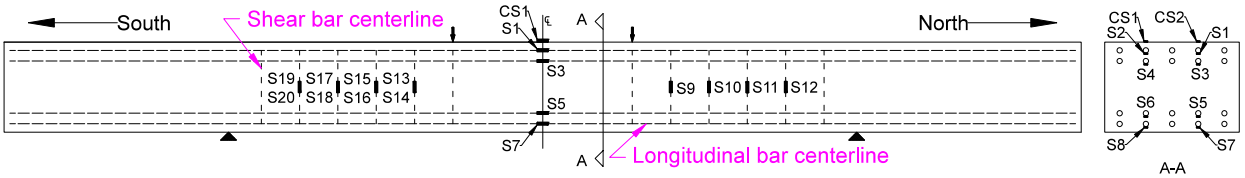

(a) Strain Gage Layout

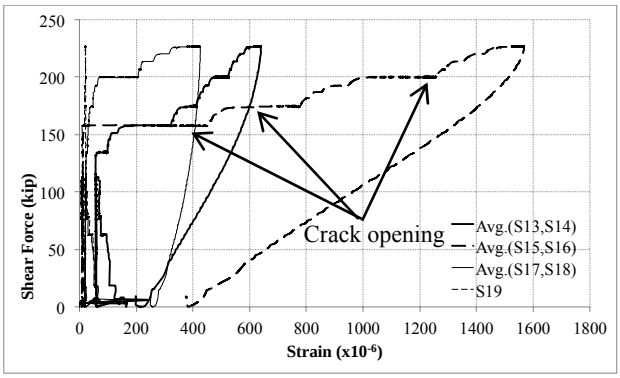

(b) 36-9T First Two Loading Cycle

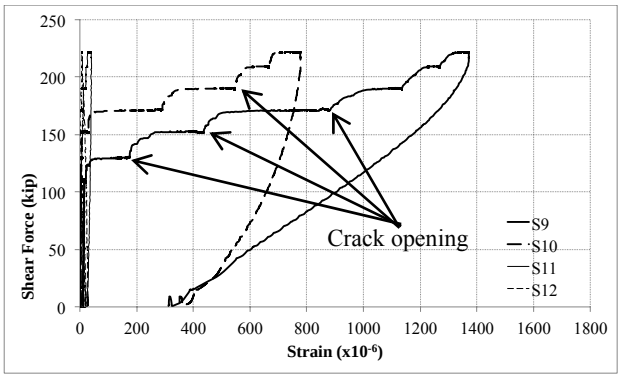

(c) 36-9S First Two Loading Cycle

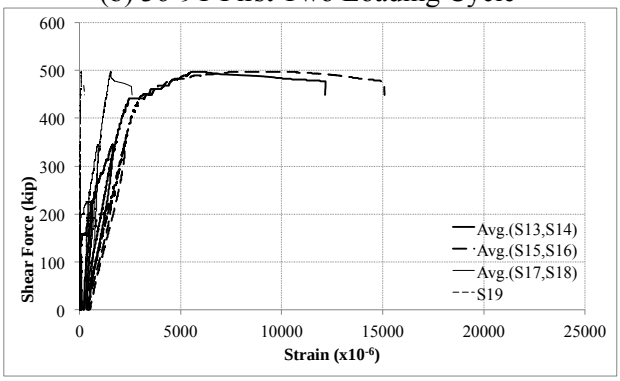

(d) 36-9T Full History

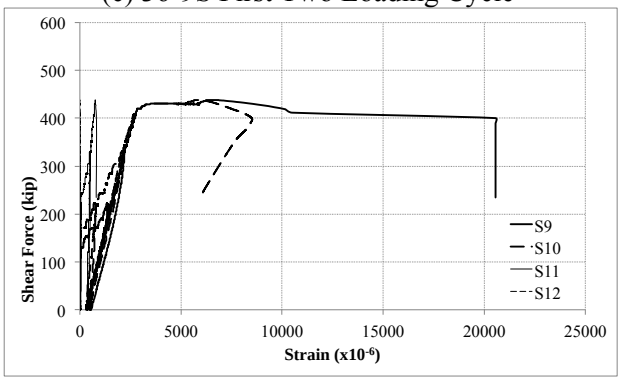

(e) 36-9S Full History

Figure 5. Strain Distribution in Shear Reinforcement

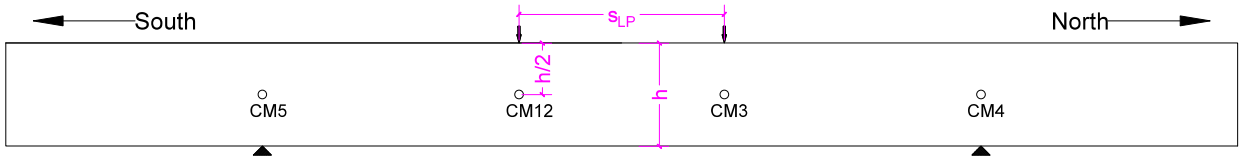

(a) Inclinometer Layout

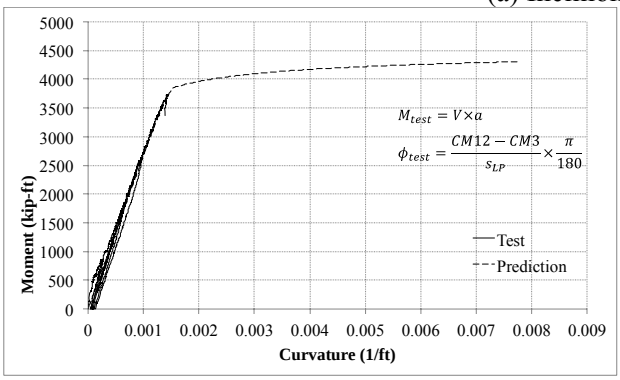

(b) 36-9T

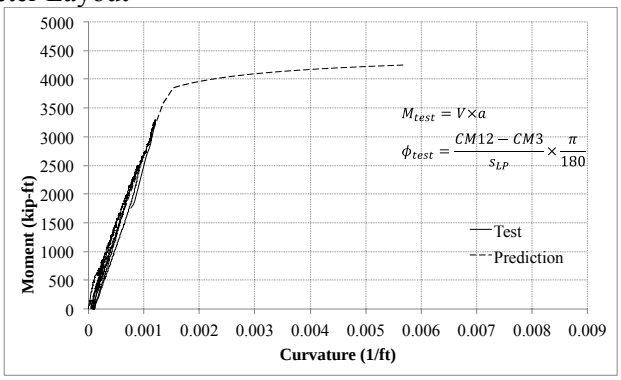

(c) 36-9S

Figure 6. Comparison of Moment-Curvature Response

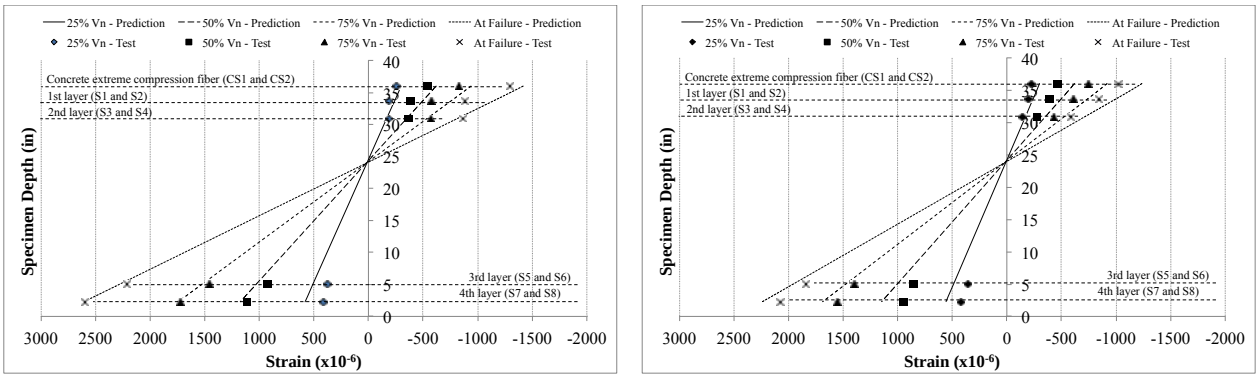

(a) 36-9T (b) 36-9S

Figure 7. Midspan Flexural Strain Profile

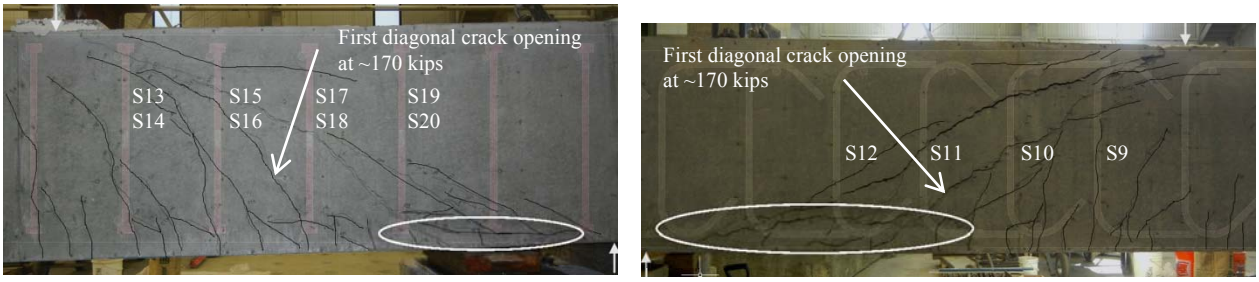

(a) 36-9T East Face (b) 36-9S East Face

(c) 36-9S Top Face (d) 36-9S Bottom Face

Figure 8. Shear Span Crack Pattern at Failure

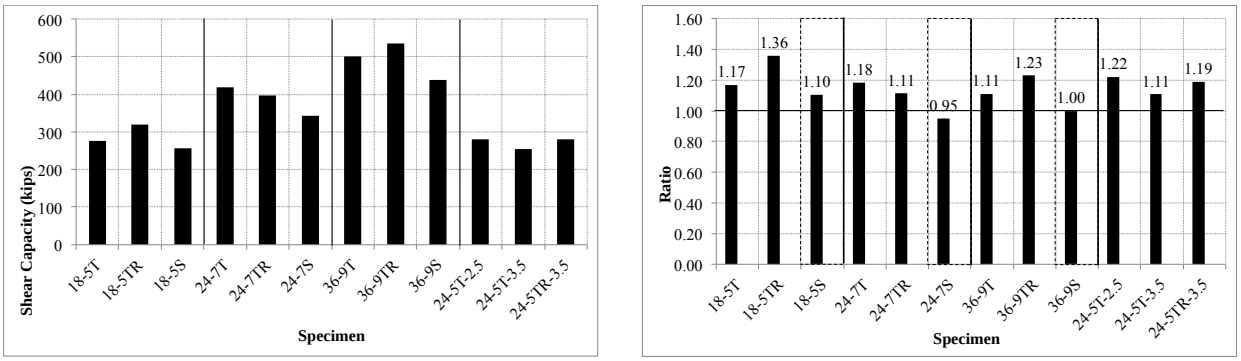

(a) Test Shear Strength (b) V_{test}/V_n^{exp}

Figure 9. Shear Strength Comparison